Available online at www.sciencedirect.com
ScienceDirect
Journal of Catalysis 254 (2008) 84–90
JOURNAL OF CATALYSIS
www.elsevier.com/locate/jcat

The benefit of mesopores in ETS-10 on the vapor-phase Beckmann rearrangement of cyclohexanone oxime

C.C. Pavel, R. Palkovits, F. Schüth, W. Schmidt *

Max-Planck-Institut für Kohlenforschung, Kaiser-Wilhelm-Platz 1, D-45470 Mülheim an der Ruhr, Germany

Received 24 October 2007; revised 28 November 2007; accepted 30 November 2007

Abstract

Mesoporosity in ETS-10 titanosilicate was generated by postsynthesis treatment with hydrogen peroxide under microwave irradiation, resulting in an increased external surface area of the materials. The influence of mesopore content, external surface area, proton-exchange conditions, and solvent on the activity of the modified ETS-10 in the Beckmann rearrangement of cyclohexanone oxime to ε-caprolactam under vapor-phase conditions was investigated. Protonated mesoporous ETS-10 was catalytically active and demonstrated improved performance with increasing external surface area.

Keywords: Beckmann rearrangement; Microporous titanosilicate; ETS-10; Mesoporosity; Structural modification

1. Introduction

The Beckmann rearrangement of cyclohexanone oxime is an important process in the production of ε-caprolactam, a valuable starting material for the manufacture of nylon-6. In the conventional industrial liquid-phase process, oleum is used as a catalyst, and large amounts of polluting ammonium sulfate are produced as a by-product. Over the last decade, numerous solid-acid catalysts, including zeolites, zeotypes, mesoporous materials, and other oxides, have been investigated to replace this environmentally unfriendly process [1,2]. MFI-type zeolites, such as high-silica ZSM-5 [3–6], TS-1 [7], and cross-linked Silicalite-1 [8], as well as BEA-type zeolite Beta [9], and FAU-type zeolite Y (USY) [10,11], are active catalysts for this process. In addition, mesoporous silica, such as FSM-16 [12] and tantalum-pillared ileride [13], are effective for the Beckmann rearrangement process. Recently, Sumitomo Chemical Co. Ltd. industrialized the production of ε-caprolactam through an environmentally friendly vapor-phase process using a high-silica MFI zeolite as a solid acid catalyst. Therein a fluidized-bed system proved advantageous in terms of catalyst regeneration [14]. Although catalytic performance over solid acid catalysts under vapor-phase conditions has been tested, the nature and position of the active sites in the catalysts remain controversial. Many researchers assume that for high-silica zeolites, hydroxyl groups of weak or intermedium acidity are the active sites that selectively form ε-caprolactam [15,16], whereas strong Brønsted acid sites favor the formation of by-products [17,18]. But discrepancies exist as to the location of the reaction sites—inside the micropores, at the pore aperture, or at the external surface of zeolite crystals [14,19–21]. Irrespective of the location of active sites, a catalyst would benefit from an increased effective diffusion coefficient if diffusion limitation were to become a crucial factor. Possible approaches to minimize diffusion limitation include either decreasing crystal size, thereby reducing the intracrystalline diffusion path length, or increasing the fraction of transport pores by introducing mesopores in a microporous material. The creation of mesopores in zeolitic materials has been shown to have a significant effect on their catalytic performance [22].

ETS-10 is a microporous titanosilicate with a three-dimensional interconnected pore system that can host exchangeable cations. The micropores are formed by 12-membered $SiO_{4/2}$ ring channels. These features make ETS-10 particularly interesting as a prospective heterogeneous catalyst [23–26]. Catalyt-

* Corresponding author. Fax: +49 208 3062995.
E-mail address: wolfgang.schmidt@mpi-muelheim.mpg.de (W. Schmidt).

0021-9517/$ – see front matter
doi:10.1016/j.jcat.2007.11.020

ically active acidic sites can be introduced in ETS-10 by forming bridging hydroxyl groups, such as Ti–(OH)–Si. As for other catalysts, the presence of structural defects affects the catalytic activity of ETS-10. In previous investigations, we found that postsynthesis treatment with hydrogen peroxide generates a hierarchical pore structure in ETS-10, which goes along with the formation of structural defects by partial leaching of Si and Ti atoms [27,28]. Well-defined mesopore channels with diameters of about 10 nm are created in ETS-10 when the treatment with H_2O_2 is performed under microwave irradiation. As a consequence, the external surface area is significantly increased [28].

This paper addresses the role of synthetically induced mesoporosity in ETS-10 on its catalytically activity in the vapor-phase Beckmann rearrangement of cyclohexanone oxime to ε-caprolactam. It also explores the influence of external surface area, ammonium exchange condition, and dilution solvent.

2. Experimental

2.1. Catalyst synthesis and modification

Well-crystallized Na,K-ETS-10 was synthesized from a gel with molar composition 1.0 Na_2O:0.2 TiO_2:0.6 KF:1.28 HCl:1.49 SiO_2:39.5 H_2O, which was stored in Teflon-lined autoclaves at a temperature of 190 °C for 3 days [29]. Mesopores were created in the titanosilicate as described previously, by treating as-synthesized ETS-10 with hydrogen peroxide under microwave irradiation [28]. Then 0.2 g of dried ETS-10 powder was mixed with 20 mL of H_2O_2 of varying concentrations and irradiated in a CEM MARS-5 microwave (MW) oven to 120 °C for 15 min. The resulting ETS-10, containing both micropores and mesopores, was recovered by filtration, washed with deionized water, and dried overnight at 80 °C. The acidity was introduced by ammonium exchange with 0.5 M NH_4NO_3 at room temperature for 15 min. Before the physicochemical and catalytic measurements, the samples thus prepared were converted into their protonated form by heating them under flowing air at 300 °C for 2 h.

2.2. Catalytic experiments

The catalytic activity of the samples in the vapor-phase Beckmann rearrangement of cyclohexanone oxime to ε-caprolactam was tested using a continuous-flow reactor packed with a mixture of 100 mg of H-ETS-10 and 2 g of quartz sand. The samples were activated overnight in an air flow at 300 °C; before the reaction, the reactor was cooled to 280 °C. Cyclohexanone oxime was dissolved in either toluene or methanol at a solvent/cyclohexanone oxime molar ratio of 26.6. This reactant was fed to the reactor by a HPLC pump with N_2 as a carrier gas. The reaction was run under atmospheric pressure with WHSV = 1.95 $g_{oxime}/(g_{catalyst}\,h)$, thus adjusting the vapor pressure of oxime to 2.2 kPa. The product was recovered by condensation of the effluent, with fractions collected for 5 min each. For analysis, three samples collected after 1 h (55, 60, 65 min) were chosen. The condensate was analyzed by a gas chromatograph equipped with a flame ionization detector (Agilent Technology 6890N).

2.3. Characterization

The ETS-10 structure was confirmed by X-ray powder diffraction (XRD) on a Stoe STADI P transmission diffractometer using Cu$K_{\alpha 1}$ radiation. The changes of the pore characteristics of the ETS-10 samples on postsynthesis treatment were studied by physical nitrogen adsorption measurements at 77 K using a Micromeritics ASAP 2010 analyzer. Before these measurements, the samples were outgassed under vacuum at 300 °C overnight. Pore size distributions were calculated with the Quantachrome Autosorb 1 software package using the nonlocal density functional theory (NLDFT) kernel for nitrogen adsorption on silica at 77 K, calculated for cylindrical pores under equilibrium conditions (desorption branch of isotherm). The external surface area of the crystallites was calculated by applying the t-plot method at the plateau of the isotherms after micropore filling. Transmission electron microscopy was done using a Hitachi 7500 transmission electron microscope operating with an acceleration voltage of 100 kV. Diffuse reflectance IR Fourier transform (DRIFT) spectra were collected with a Nicolet Magna-IR 560 spectrometer with a spectral resolution of 2 cm^{-1}. The samples were preheated at 280 °C in a stream of N_2 gas for 2 h inside an IR cell to achieve complete dehydration. For pyridine adsorption experiments, the dehydrated samples were exposed to a saturated vapor flow for 1 h at 25 °C. The desorption of pyridine was carried out stepwise at 25, 100, 200, 280, and 350 °C for 1 h at each temperature.

3. Results and discussion

Crystalline microporous materials generally have a narrow pore size distribution characterized by type I isotherms. Fig. 1 presents the nitrogen adsorption isotherms of as-synthesized and ETS-10 treated with H_2O_2 under microwave irradiation. As-made ETS-10 shows a typical type I isotherm indicating a fully microporous material. After microwave-assisted H_2O_2 treatment, the uptake of N_2 at higher relative pressures is increased significantly and is accompanied by a hysteresis loop. This indicates the presence of an additional mesopore system in this material. The pore size distributions derived from the N_2 adsorption branches of the isotherms were calculated using procedures based on the NLDFT method. These distributions show the formation of mesopores in the H_2O_2-treated material, with an average pore size of about 6.5 nm (Fig. 1, insert). The presence of mesopores contributes to the external surface area. Indeed, the external surface area of the crystallites after hydrogen peroxide treatment, as calculated by the t-plot method, increased from 8.5 $m^2\,g^{-1}$ for as-synthesized ETS-10 to 70 $m^2\,g^{-1}$ for meso-ETS-10. Fig. 2 shows the TEM image of a mesoporous ETS-10 sample. The bright areas in the picture represent mesoporous cavities within the materials. Based on the TEM micrograph, they appear to be 6–7 nm in size, which is in good agreement with the pore size distribution derived from nitrogen sorption experiments.

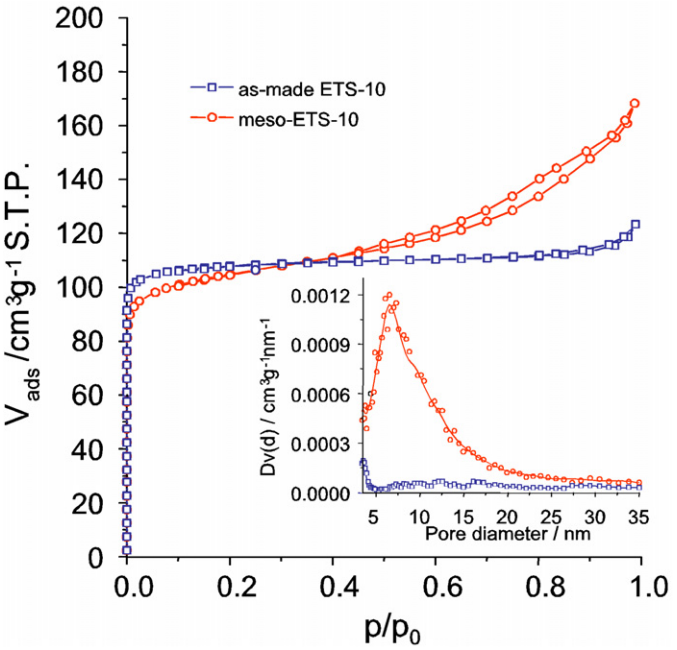

Fig. 1. Nitrogen adsorption isotherms of as-synthesized Na,K-ETS-10 and hydrogen peroxide-treated ETS-10 under microwave irradiation and their pore size distribution in mesoporous range (insert).

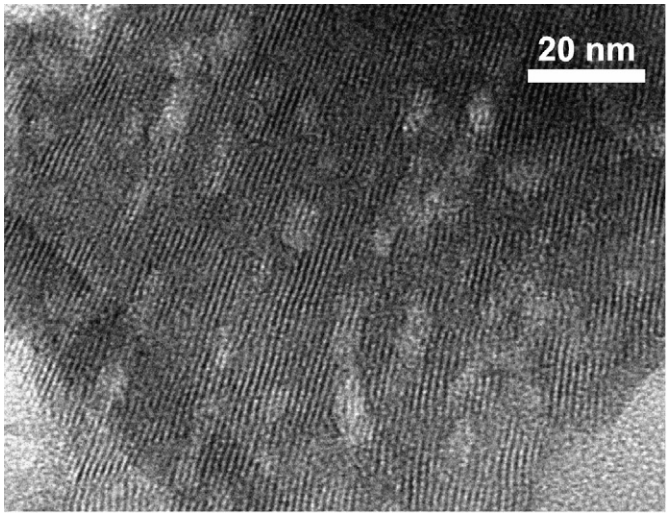

Fig. 2. TEM image of hydrogen peroxide-treated ETS-10 under microwave irradiation.

Another effect of the microwave-assisted H_2O_2 treatment was the formation of additional silanol groups. This was confirmed by IR spectra recorded in the region of O–H stretching vibrations. The DRIFT spectra obtained at 2600–4000 cm^{-1} are displayed in Fig. 3. After in-situ dehydration at 300 °C under N_2 flow, the as-synthesized ETS-10 exhibited two distinct adsorption bands at 3730 and 3701 cm^{-1}. A third broad band was centered at 3507 cm^{-1} (Fig. 3). There are little data in the literature on the assignment of IR bands in the O–H stretching region of ETS-10 materials; however, the bands at 3730 and 3701 cm^{-1} appear to correspond to isolated Si–OH and Ti–OH groups, respectively. The broad band at 3600–3400 cm^{-1} has been tentatively assigned to H-bridged surface hydroxyl groups

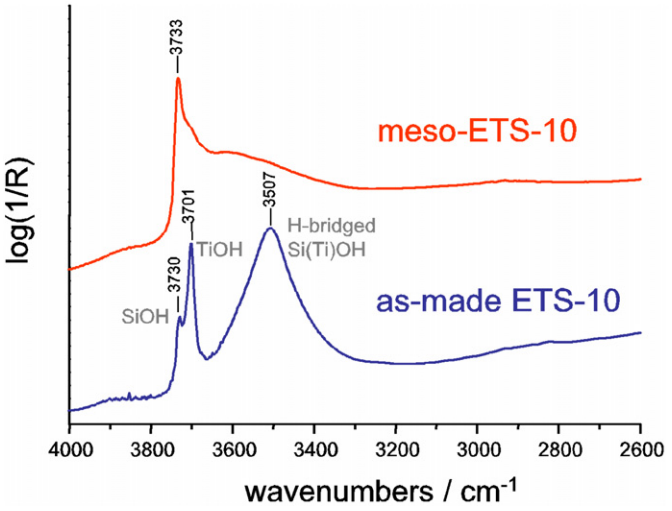

Fig. 3. DRIFT spectra of dehydrated as-synthesized ETS-10 and mesopores-containing ETS-10.

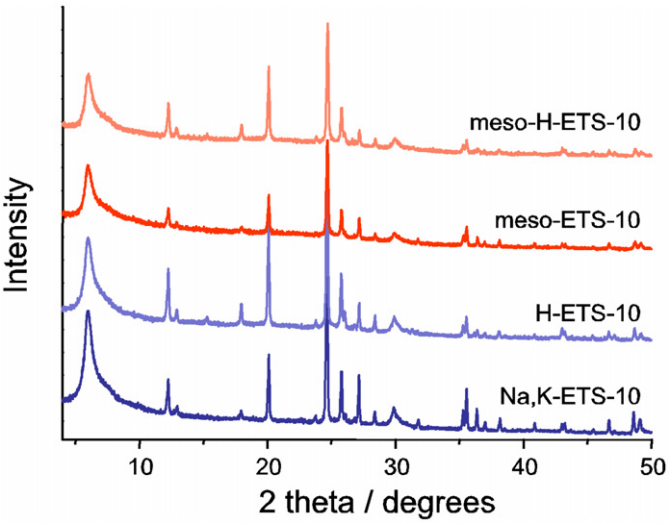

Fig. 4. XRD powder patterns of different ETS-10 and meso-ETS-10 samples.

of both Si and Ti atoms [27,30,31]. After H_2O_2 treatment, the band attributed to Si–OH groups increased considerably in intensity (Fig. 3). Apparently, the new silanol groups created by the partial leaching of Ti and Si atoms would be located not only on the external surface of crystallites, but also on the walls of mesopores generated by the postsynthesis treatment [27].

Proton exchange of microporous and mesoporous samples was achieved by ammonium exchange with NH_4NO_3 at room temperature, followed by heating in flowing air at 300 °C. During this procedure, the crystallinity of the samples, designated H-ETS-10 and meso-H-ETS-10, was well preserved, as indicated by their XRD patterns (Fig. 4). The samples, mounted between two polymer foils, were measured in transmission mode; thus, samples of different thicknesses produced somewhat differing absolute reflection intensities and signal-to-noise ratios. As expected, protonation of ETS-10 by ammonia exchange and calcination resulted in significant changes in the XRD patterns. This finding held for both the as-made NaK-ETS-10 and meso-

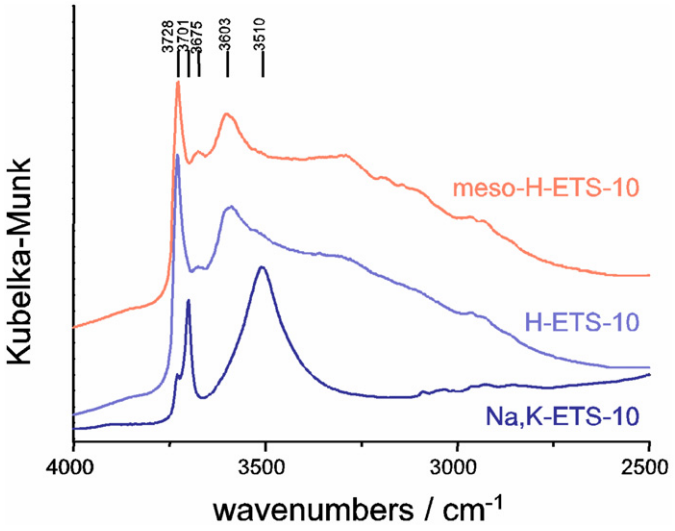

Fig. 5. DRIFT spectra of the dehydrated as-synthesized ETS-10, H-ETS-10, and mesopores-containing H-ETS-10.

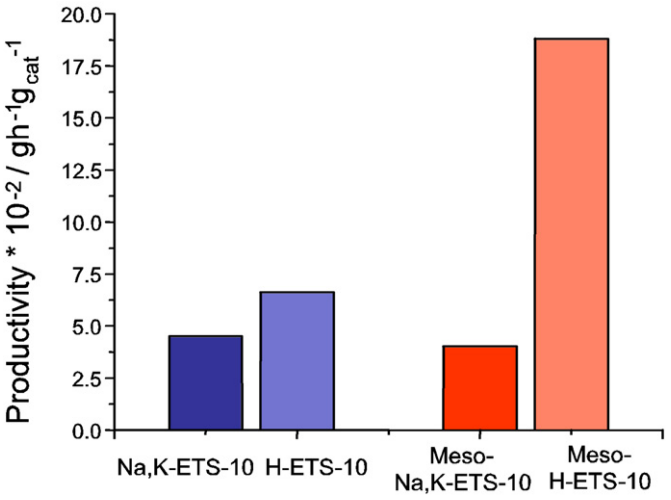

Fig. 6. Reaction rate to Beckmann rearrangement of cyclohexanone oxime for acidic and nonacidic micropores- and mesopores-containing ETS-10 samples.

ETS-10. However, the crystallinities of the samples as measured by XRD seemed not to be strongly affected by H_2O_2 treatment. The IR spectra changed significantly once the protons were introduced in the ETS-10 materials. Fig. 5 displays the DRIFT spectra, obtained in the range 2500–4000 cm^{-1}, along with the spectrum of as-synthesized Na,K-ETS-10 for comparison. The protonated forms of both samples show two main bands at 3728 and 3603 cm^{-1}. Comparing these with the well-established assignments of the fundamental stretching bands of the proton form of aluminosilicate zeolites [32], we tentatively assign the two bands as follows. The first band, at 3728 cm^{-1}, which also is visible in the spectrum of as-synthesized ETS-10, is most likely due to the fundamental stretch of silanol groups [Si–OH] located at either the crystallite surfaces or at crystal defects. The second band, at 3603 cm^{-1}, most likely corresponds to the fundamental stretching mode of bridging hydroxyls, such as Ti–(OH)–Si groups. Such bridging hydroxyl groups are most important for the performance of zeolitic catalysts, because they are directly associated with their acidity and thus are responsible for their catalytic activities.

The generation of a hierarchical pore system in ETS-10 leads to an increase of the external surface area, and thus it should have a positive effect on the catalytic activity of reactions occurring preferentially at or close to the external crystal surfaces of the catalyst particles. Consequently, we tested the ETS-10 samples as catalysts for the vapor-phase Beckmann rearrangement of cyclohexanone oxime to ε-caprolactam (CL). First set of catalytic reactions used toluene as the solvent. Fig. 6 shows the reaction rates of the native (Na, K) and protonated forms of the ETS-10 and meso-ETS-10 samples. For the H-ETS-10 sample, a reaction rate of 6.65×10^{-2} $g_{CL}/(g_{ETS}\,h)$ with a selectivity >76% was observed. For meso-H-ETS-10, the reaction rate increased almost three-fold, to 18.8×10^{-2} $g_{CL}/(g_{ETS}\,h)$, demonstrating similar selectivity as the microporous H-ETS-10. The introduction of mesopores in ETS-10 clearly had a beneficial effect on the catalytic performance. Both micro- and meso-Na,K-ETS-10 showed low selectivity for ε-caprolactam, with reaction rates not exceeding 4.5×10^{-2} $g_{CL}/(g_{ETS}\,h)$, which could be attributed to a decreased proton-donating ability and correspondingly lower acidity. These materials contain only weakly acidic silanol and titanol groups at their external surfaces and, for the H_2O_2-treated sample, within the mesopores.

Accordingly, a major factor in the enhanced catalytic performance of mesoporous ETS-10 in the vapor-phase Beckmann rearrangement reaction seems to be not only the presence of mesopores, but also the acidity of newly created Brønsted acid sites interplaying with the intracrystalline chemical environment of the titanosilicate.

Several studies have reported an advantageous impact of methanol as solvent in the reaction [9,34,35]. Their findings led to the conclusion that desorption of ε-caprolactam seems to be the rate-determining step in the reaction [34]. Thus, the polarity of methanol or other alcohols might enhance product release, resulting in an overall increased reaction rate. Simultaneously, higher selectivities toward ε-caprolactam have been reported and explained by formation of methoxy groups on the catalyst surface [14,36]. It was concluded that mainly strong acidic sites formed methoxy groups, whereas the remaining sites of medium and low acidity led to a high selectivity toward ε-caprolactam. Consequently, in a second set of reactions, the acidic forms of microporous and mesoporous ETS-10 samples were tested using methanol as the solvent, with all other reaction parameters kept identical. In the presence of methanol, the productivity (reaction rate) of microporous H-ETS-10 remained almost unchanged (6.85×10^{-2} $g_{CL}/(g_{ETS}\,h)$), with a selectivity of 69%. Surprisingly, meso-H-ETS-10 showed a significantly decreased productivity of only to 8.5×10^{-2} $g_{CL}/(g_{ETS}\,h)$, with a maximum selectivity of 50%. This somewhat unexpected behavior may be explained by the low acidity of the catalytically active sites in ETS-10. Consequently, desorption of caprolactam may not be enhanced by methanol, and methoxy groups leading to improved selectivity may not be formed. Using ETS-10 as the catalyst may require different reaction conditions to optimize productivity compared with other intensively investigated solid acid cata-

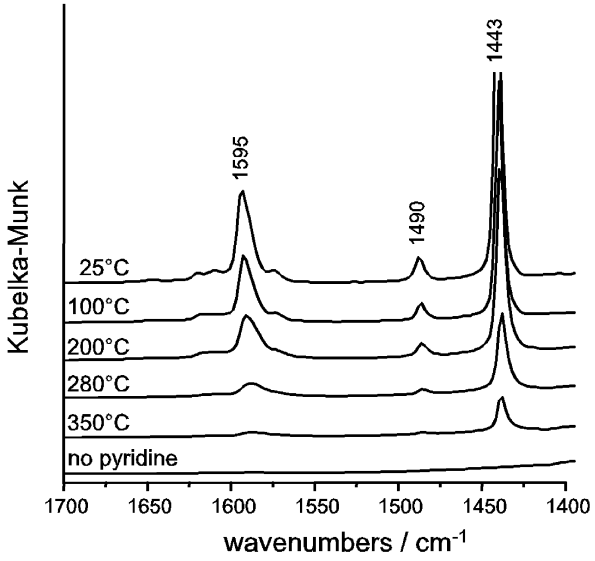

Fig. 7. Diffuse reflectance IR spectra of as-synthesized Na,K-ETS-10 (bottom) and Na,K-ETS-10 after pyridine adsorption and heating from 25 to 350 °C.

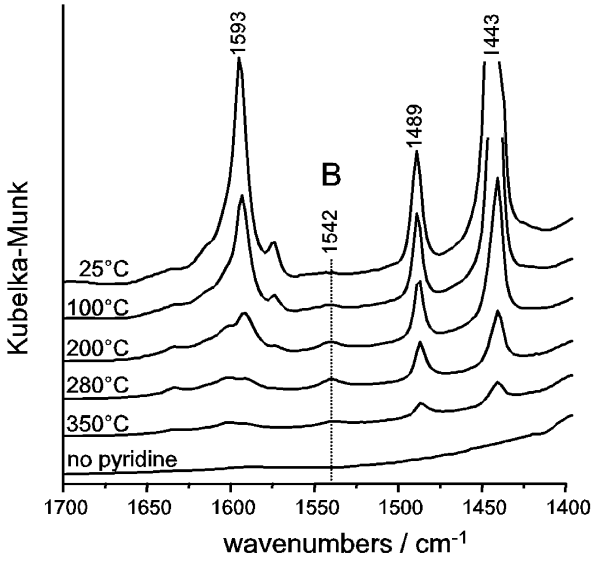

Fig. 8. Diffuse reflectance IR spectra of H-ETS-10 (bottom) and H-ETS-10 after pyridine adsorption and heating from 25 to 350 °C.

lysts for this reaction. However, the catalytic results reveal a strong correlation among newly created mesoporosity of the ETS-10 samples, the resulting mesopore areas, and the catalytic activities of the materials. Moreover, the acidity of the catalytically active sites seems to be crucial for a high selectivity.

To evaluate the acidic properties of the materials, such as the presence and strength of Brønsted acid sites on the external and internal surface of ETS-10 crystallites, IR studies were performed using pyridine as the probe molecule. The IR frequencies of pyridine interacting with acidic sites and their assignments are rather well known for aluminosilicate zeolites. Pyridinium ions, formed by protonation of pyridine molecules after reacting with Brønsted acid sites, show an IR band at about 1540 cm^{-1}. Figs. 7–9 show the DRIFT spectra of pyridine adsorbed on as-synthesized ETS-10, micro-H-ETS-10, and

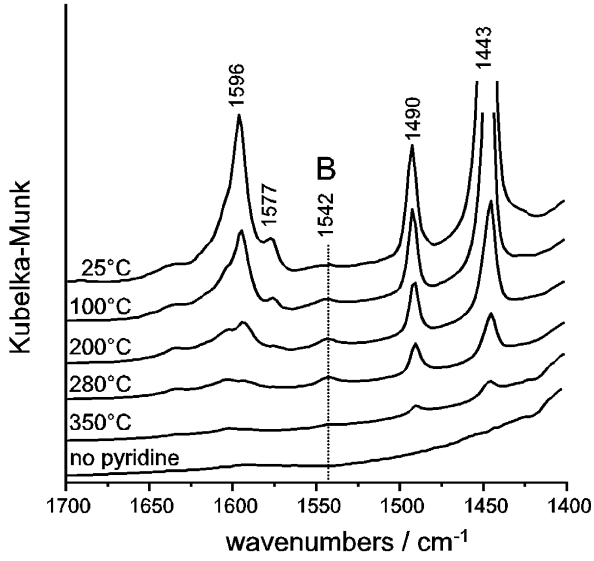

Fig. 9. Diffuse reflectance IR spectra of meso-H-ETS-10 (bottom) and meso-H-ETS-10 after pyridine adsorption and heating from 25 to 350 °C.

meso-H-ETS-10 samples at 25 °C and after heat treatment at different temperatures. After outgassing at 280 °C, the spectra of all ETS-10 samples do not show any significant IR absorption in the range of 1400–1700 cm^{-1} (spectra labeled as "no pyridine" in Figs. 7–9). Immediately after cooling to room temperature and exposure to pyridine flow, the spectrum of as-synthesized Na,K-ETS-10 shows three main peaks at 1595, 1490, and 1443 cm^{-1} and a weak band at 1577 cm^{-1} (spectrum labeled as "25 °C" in Fig. 7). Comparing these with specific IR bands of pyridine adsorbed on aluminosilicates zeolites [32] led to the following assignments: The most intense signal at 1443 is ascribed to pyridine attached to Na^+ and K^+ cations; the other IR bands cannot be attributed precisely and represent so-called "unspecifically" adsorbed pyridine. The spectra of the proton forms of microporous and mesoporous ETS-10 samples exhibit almost identical IR bands (Figs. 8 and 9). The signal at 1443 cm^{-1} is still visible, demonstrating that the ammonium-exchange process was not completed. However, a new IR band at 1542 cm^{-1} appears in the spectra of protonated-ETS-10 samples. This band is indicative of the presence of Brønsted acid sites (B-sites) on the external and internal surfaces of proton-exchanged ETS-10 samples. On heating to 350 °C, the band at 1542 cm^{-1} remains nearly constant for both proton-exchanged samples, whereas the other peaks decrease in intensity (Figs. 8 and 9). The nature of the acidity in ETS-10 remains incompletely understood. Using acidity tests, Liepold et al. have found that the catalytically active species on Al-containing ETS-10 are indeed the bridging hydroxyl groups of type Ti–(OH)–Si [33]. Thus, we assume that the same type of site is responsible for the Brønsted acidity of the protonated ETS-10 samples under investigation.

We found that ammonium-exchange conditions had no significant effect on the catalytic activity of ETS-10. The catalytic activity remained more or less unchanged irrespective of the exchange procedure applied. Thus, samples on which the ion exchange had been performed at 50 °C for 12 h and those that had

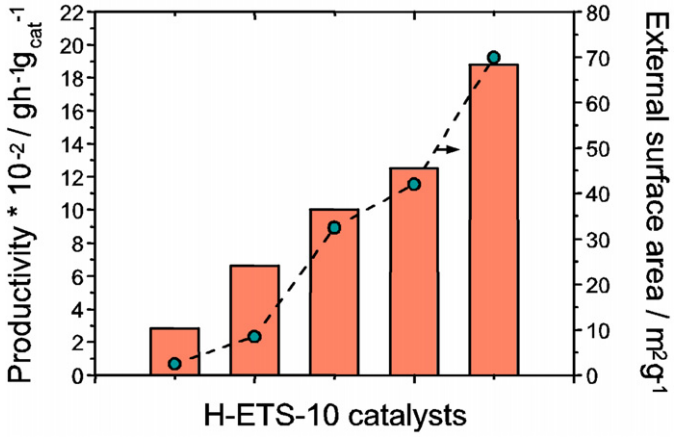

Fig. 10. Catalytic activity in Beckmann rearrangement of cyclohexanone oxime reaction and external surface areas of various H-ETS-10 samples.

been exchanged several times with fresh ammonium solution showed almost identical activity. The only effect observed after extended ion exchange or exchange at elevated temperature was a significant decrease in the crystallinity of the samples. Short contacts of ETS-10 with ammonium-containing solutions resulted in a sufficient exchange of the parent Na and K cations.

Recently we reported that the mesopore volumes in ETS-10 can be controlled by varying the concentration of the hydrogen peroxide used for the postsynthesis treatment and the temperature induced by the microwaves [28]. We tested various H-ETS-10 samples containing different amounts of mesopores and thus different surface areas in the Beckmann rearrangement reaction. Fig. 10 compares the caprolactam productivity of the different samples, as well as the external surface areas of the respective meso-H-ETS-10 samples. The crystallite size range was identical (0.5–1.0 μm) in all samples except the first sample shown in Fig. 10, which consisted of somewhat larger crystallites (3–5 μm) and thus had a smaller external surface area than the second sample, which is identical to the H-ETS-10 sample shown in Fig. 6. The last three samples were treated with H_2O_2 to create mesopores. The ammonium-exchange conditions and calcination process were kept identical for all samples. As can be seen in Fig. 10, there is a correlation between the catalytic activity and the external surface area, with increased catalytic activity with increasing mesopore area.

The pores of ETS-10 are sufficiently large to allow cyclohexanone oxime to enter the micropores. Thus, the catalytic conversion proceeds not only on the external surface area, but also probably inside the pores of ETS-10. Therefore, a linear dependence of the productivity from on the external surface area would be not expected for materials with low external surface areas. Then the catalytic conversion would be dominated most likely by mass transfer into the micropores. When larger mesopores are present in significant amounts, the surface contribution becomes more dominant and the productivity indeed then scales with the external surface area (e.g., 1×10^{-1} g h^{-1} g$_{cat}^{-1}$ for a material with an external surface area of about 33 m^2 g^{-1} and 1.9×10^{-1} g h^{-1} g$_{cat}^{-1}$ for a material with an external surface area of about 70 m^2 g^{-1}). Along with the impact of Brønsted acid sites, the presence of mesopores strongly enhances the catalytic activity of ETS-10 for the Beckmann rearrangement of cyclohexanone oxime. Thus, it can be assumed that the reaction might proceed mainly at the external surface of the ETS-10 crystallites. Nonetheless, a possible beneficial effect from decreased diffusion limitation due to the presence of larger transport pores cannot be excluded. Excluding the effect of mass transfer limitation would require independent diffusion measurements, as have been carried out for hydroisomerization of hexane over Pt/MOR [37].

4. Conclusion

A hierarchical porosity can be induced in ETS-10 by treatment with hydrogen peroxide under microwave irradiation. Partial leaching of Ti and Si atoms results in a certain mesoporosity of the crystallites. The crystallinity of H-ETS-10 catalysts is well preserved if the protonation is performed while keeping the contact times with ammonium nitrate solution rather short. The protonated forms of ETS-10 were found to be active in the vapor-phase Beckmann rearrangement of cyclohexanone oxime, especially when toluene was used as the solvent. The greatest productivity for ε-caprolactam (18.8×10^{-2} g$_{CL}$/(g$_{ETS}$ h)) was achieved with a H-ETS-10 sample with a high concentration of mesopores, resulting in a total external surface area of about 70 m^2 g^{-1}. The catalytically active species in rearrangement of cyclohexanone oxime to ε-caprolactam are most likely Brønsted-acidic bridging hydroxyl groups (Ti–(OH)–Si). The catalytic activity is strongly correlated with the external surface area of meso-H-ETS-10 titanosilicate samples.

References

[1] G. Dalhhoff, J.P.M. Niederer, W.F. Hölderich, Catal. Rev.-Sci. Eng. 43 (2001) 827.
[2] T. Tatsumi, in: R.A. Sheldon, H. van Bekkum (Eds.), Fine Chemicals through Heterogeneous Catalysis, Wiley–VCH, 2001, p. 185.
[3] H. Sato, K. Hirose, N. Ishii, Y. Umeda, US Patent 4,709,024 (1987) to Sumitomo Chemical Co. Ltd.
[4] H. Ichihashi, M. Kitamura, Catal. Today 73 (2002) 23.
[5] T. Takahashi, T. Kai, E. Nakao, Appl. Catal. A Gen. 262 (2004) 137.
[6] L. Forni, G. Fornasari, G. Giordano, C. Lucarelli, A. Katovic, F. Trifirò, C. Perri, J.B. Nagy, Phys. Chem. Chem. Phys. 6 (2004) 1842.
[7] H. Ichihashi, H. Sato, Appl. Catal. A Gen. 221 (2001) 359.
[8] R. Palkovits, Y. Ilhan, W. Schmidt, C.M. Yang, A. Erdem-Sentalar, F. Schüth, Stud. Surf. Sci. Catal. 158 (2005) 1255.
[9] L.X. Dai, R. Hayasaka, Y. Iwaki, K. Koyama, T. Tatsumi, Chem. Commun. (1996) 1071.
[10] C. Ngamcharussrivichai, P. Wu, T. Tatsumi, J. Catal. 235 (2005) 139.
[11] C. Ngamcharussrivichai, P. Wu, T. Tatsumi, Appl. Catal. A Gen. 288 (2005) 158.
[12] D. Shouro, Y. Moriya, T. Nakajima, S. Mishima, Appl. Catal. A Gen. 198 (2000) 275.
[13] Y. Ko, M.H. Kim, Y.S. Uh, Chem. Commun. (2000) 829.
[14] H. Ichihashi, M. Ishida, A. Shiga, M. Kitamura, T. Suzuki, K. Suenobu, K. Sugita, Catal. Surv. Jpn. 7 (2003) 261.
[15] G.P. Heitmann, G. Dahlhoff, W.F. Hölderich, Appl. Catal. A Gen. 185 (1999) 99.
[16] G.P. Heitmann, G. Dahlhoff, W.F. Hölderich, J. Catal. 186 (1999) 12.
[17] S. Sato, S. Hasabe, H. Sakurai, K. Urabe, Y. Izumi, Appl. Catal. 29 (1987) 107.
[18] T. Ushikubo, K. Wada, J. Catal. 148 (1994) 138.

[19] H. Kath, R. Gläser, J. Weitkamp, Chem. Eng. Technol. 24 (2001) 150.
[20] M.A. Camblor, A. Corma, H. García, V. Semmer-Herlédan, S. Valencia, J. Catal. 177 (1998) 267.
[21] H. Sato, Catal. Rev.-Sci. Eng. 39 (1997) 395.
[22] S. van Donk, A.H. Janssen, J.H. Bitter, K.P. de Jong, Catal. Rev. 45 (2003) 297;
Y. Tao, H. Kanoh, L. Abrams, K. Kaneko, Chem. Rev. 106 (2006) 896.
[23] S.M. Kuznicki, US Patent 4,853,202 (1989) to Engelhard Corporation.
[24] M.W. Anderson, O. Terasaki, T. Ohsuna, A. Philippou, S.P. MacKay, A. Ferreira, J. Rocha, S. Lidin, Nature 367 (1994) 347.
[25] M.W. Anderson, O. Terasaki, T. Ohsuna, P.J.O. Malley, A. Philippou, S.P. MacKay, A. Ferreira, J. Rocha, S. Lidin, Philos. Mag. B 71 (1995) 813.
[26] J. Rocha, M.W. Anderson, Eur. J. Inorg. Chem. (2000) 801.
[27] C.C. Pavel, S.-H. Park, A. Dreier, B. Tesche, W. Schmidt, Chem. Mater. 18 (2006) 3813.
[28] C.C. Pavel, W. Schmidt, Chem. Commun. (2006) 882.
[29] C.C. Pavel, D. Vuono, L. Catanzaro, P. De Luca, N. Bilba, A. Nastro, J.B. Nagy, Microporous Mesoporous Mater. 56 (2002) 227.
[30] R. Robert, P.R. Rajamohanan, S.G. Hegde, A.J. Chandwadkar, P. Ratnasamy, J. Catal. 155 (1995) 345.
[31] A. Zecchina, F.X. Llabrés i Xamena, C. Pazè, G.T. Palomino, S. Bordiga, C.O. Areán, Phys. Chem. Chem. Phys. 3 (2001) 1228.
[32] H.G. Karge, M. Hunger, H.K. Beyer, in: J. Weitkamp, L. Puppe (Eds.), Catalysis and Zeolites, Springer-Verlag, 1998, pp. 198–326.
[33] A. Liepold, K. Roos, W. Reschetilowski, Z. Lin, J. Rocha, A. Philoppou, M.W. Anderson, Microporous Mater. 10 (1997) 211.
[34] T. Komatsu, T. Maeda, T. Yashima, Microporous Mesoporous Mater. 35 (2000) 173.
[35] T. Yashima, N. Oka, T. Komatsu, Catal. Today 38 (1997) 249.
[36] M. Kitamura, H. Ichihashi, Stud. Surf. Sci. Catal. 90 (1994) 67.
[37] S. van Donk, A. Broersma, O.L.J. Gijzeman, J.A. van Bokhoven, J.H. Bitter, K.P. de Jong, J. Catal. 204 (2001) 272.